Pflügers Arch - Eur J Physiol (2001) 442:577–587
DOI 10.1007/s004240100567

ORIGINAL ARTICLE

G. Glassmeier · M. Hauber · I. Wulfsen
F. Weinsberg · C. K. Bauer · J. R. Schwarz

Ca^{2+} channels in clonal rat anterior pituitary cells (GH_3/B_6)

Received: 23 October 2000 / Received after revision: 29 January 2001 / Accepted: 7 March 2001 / Published online: 17 May 2001

Abstract In clonal rat somatomammotroph cells (GH_3/B_6) Ca^{2+} influx through voltage-dependent Ca^{2+} channels is important for regulating the Ca^{2+} concentration that mediates hormone secretion. To study the Ca^{2+} channel subtypes in GH_3/B_6 cells, Ca^{2+} channel currents were recorded with the whole-cell configuration of the patch-clamp technique using Ba^{2+} as the charge carrier. Forty-nine percent of the total Ba^{2+} current amplitude was mediated by a nifedipine-sensitive current (L-type). In addition, three other high-voltage-activated Ca^{2+} channel current components could be distinguished pharmacologically: 10 nM ω-agatoxin-IVA-sensitive current (22%; P-type), ω-conotoxin-MVIIC-sensitive current (18%; Q-type), and toxin-resistant current (24%). Since ω-conotoxin GVIA (2 µM) had no blocking effect, N-type Ca^{2+} channels are assumed not to be present in GH_3/B_6 cells. The T-type Ca^{2+} channel current was either absent or very small. Different pore-forming α_1 subunits of Ca^{2+} channels were found to be expressed in GH_3/B_6 cells, which could be the molecular correlates of the different Ba^{2+} current subtypes: α_{1G} of T-type, α_{1C}, α_{1D} and α_{1S} of L-type, and α_{1A} of P/Q-type current. In addition, transcripts for β1, β2 and β3 subunits were detected. Blockage of L-type channels with 10 µM nifedipine or P/Q-type channels with 10 nM ω-agatoxin MVIIC + 200 nM ω-conotoxin blocked action potential firing in GH_3/B_6 cells and decreased basal prolactin secretion.

Keywords ω-Agatoxin IVA · Ca^{2+} channels · ω-Conotoxin MVIIC · GH_3/B_6 cells · Nifedipine · Patch-clamp · Prolactin secretion · Reverse hemolytic plaque assay · RT-PCR

G. Glassmeier · M. Hauber · I. Wulfsen · F. Weinsberg
C.K. Bauer · J.R. Schwarz (✉)
Abteilung für Angewandte Physiologie,
Institut für Physiologie,
Universitätsklinikum Hamburg-Eppendorf,
Martinistr. 52, 20246 Hamburg, Germany
e-mail: schwarz@uke.uni-hamburg.de
Tel.: +49-40-428032190, Fax: +49-40-428039127

Introduction

GH_3/B_6 and GH_3 cells are clonal somatomammotroph cells that have been used to study the cellular mechanisms underlying prolactin secretion [14]. As in other neuroendocrine cells, hormone secretion from GH cells is regulated by the free intracellular Ca^{2+} concentration ($[Ca^{2+}]_i$), which is mainly controlled by an influx of Ca^{2+} through voltage-dependent Ca^{2+} channels. Low-voltage-activated (LVA) and high-voltage-activated (HVA) Ca^{2+} channels have been distinguished in GH_3 cells [30, 32, 44, 48]. Both types of Ca^{2+} current have also been described in various native pituitary cells (reviewed in [14]). LVA Ca^{2+} channels activate at potentials more positive than –60 mV and mediate transient currents (T-type), whereas HVA Ca^{2+} channels activate at potentials more positive than –40 mV and mediate slowly or non-inactivating Ca^{2+} currents. HVA Ca^{2+} channels have been divided into five different subtypes based on their distinct pharmacological properties [36, 37, 42, 54]: L-type channels are blocked by dihydropyridines (DHP), P-type channels by low concentrations of ω-agatoxin IVA (<10 nM), Q-type channels by high concentrations of ω-agatoxin IVA (>100 nM) or ω-conotoxin MVIIC, and N-type channels by ω-conotoxin GVIA. R-type channels are characterized by their resistance to all of these blockers. With the help of these selective toxins it has been shown that in corticotrophs [21] and melanotrophs [12] the HVA current is composed of different Ca^{2+} current subtypes. This may also be the case in GH_3/B_6 cells, because in GH_3 cells only part of the HVA Ca^{2+} current is blocked by DHPs [1, 9].

Ca^{2+} channels consist of a pore-forming α_1 subunit and additional modulating subunits [42, 54]. To identify the different Ca^{2+} channels in GH_3/B_6 cells, we performed electrophysiological and pharmacological experiments to distinguish the different Ca^{2+} channel subtypes and tried to correlate these subtypes to the different α_1 subunits detected with RT-PCR. In addition to a small T-type current, four HVA Ca^{2+} current components were present in GH_3/B_6 cells: L-, P-, Q-type and toxin-resis-

tant currents. Possible molecular correlates of the pore-forming α_1 subunits were found to all but the toxin-resistant current. Upon blockage of L-type or P/Q-type Ca^{2+} channels, the firing of action potentials ceased and basal prolactin secretion decreased.

Materials and methods

Cell culture

GH_3/B_6 cells were grown as monolayers in Ham's F10 medium (Sigma) supplemented with 15% horse serum (Gibco), 2.5% fetal calf serum (Biother) and 0.5% L-glutamine (Sigma). The cell cultures were maintained at 37°C in a humidified atmosphere of 95% air and 5% CO_2. The medium was changed every 2–3 days and cells were passaged as they reached confluence, usually once a week. For the electrophysiological recordings cells were plated in 35-mm plastic culture dishes (Nunc).

Electrophysiology

Recordings were made 1–6 days after plating. Membrane currents were recorded in the whole-cell configuration of the patch-clamp technique [17], using an EPC9 patch-clamp amplifier and PULSE/PULSE FIT software (HEKA Elektronik, Lambrecht, Germany). Action potentials were recorded with the nystatin-perforated-patch configuration [18] using an EPC7 patch-clamp amplifier and SPIKE2 software (Cambridge Electronic Design, Cambridge, UK). Pipettes filled with intracellular solution had resistances in the range of 2–4 MΩ. Series resistance errors were compensated up to 60–80%. Experiments were performed at room temperature (22–25°C). In the perforated-patch configuration the pipettes were filled with intracellular solution containing nystatin (200 µg/ml). Nystatin was dissolved in dimethyl sulphoxide (DMSO), and the final DMSO concentration did not exceed 0.2%.

Solutions

Ca^{2+} channel currents were recorded in an external solution containing (in mM): NaCl 130, $MgCl_2$ 1.2, $BaCl_2$ 10, HEPES 10. To this solution tetrodotoxin (TTX, 500 nM) was added. The pH was adjusted to 7.3 with NaOH. The pipette solution in these experiments was (in mM): CsCl 135, $MgCl_2$ 2, HEPES 10, EGTA 10, Mg-ATP 4; pH adjusted to 7.3 with TEA-OH. The extracellular solution used in the current-clamp experiments contained (in mM): NaCl 135, KCl 5, $MgCl_2$ 2, $CaCl_2$ 2, HEPES 10, glucose 10, pH adjusted to 7.3 with NaOH. The pipette solution to which nystatin was added contained: KCl 140, $MgCl_2$ 4, $CaCl_2$ 1, EGTA 2.5, HEPES 10, pH adjusted to 7.3 with KOH. Drugs were applied using a superfusion system by switching from drug-free control solution to drug-containing solution or using application by pipetting the drugs directly into the bath.

RT-PCR of GH_3/B_6 cells

RNAs were extracted from GH_3/B_6 cells using RNAzol™ B (AGS, Heidelberg, Germany) [11]. DNase digestion was performed routinely before preparing cDNA. One microgram of total RNA was employed for oligo (dT) primed reverse transcription using M-MLV reverse transcriptase (Gibco). The cDNAs were amplified with 1.25 U of *Taq* DNA polymerase (Stratagene), 1.5 mM $MgCl_2$ and 0.2 mM of each dNTP in 50-µl reaction assays using 5 pmol of forward and reverse oligonucleotide primers specific for the different Ca^{2+} channel α_1 and β subunit cDNAs (see

Table 1 Oligonucleotide sequences of primer pairs used for RT-PCR of voltage-dependent Ca^{2+} channel α_1 and β subunits

Subunit	Primer sequence	RT-PCR product	Accession no.	Reference
α_{1A}	5′-CACCAACCCTGGTCCCGCCT-3′ 5′-CATGGGCTTTGGGCCATCCT-3′	333 bp	M64373	[53]
α_{1B}	5′-AAAGCACAGAGCTTCTACTG-3′ 5′-GTGGTTGGAGTCTCATCTTG-3′	474 bp	M92905	[15]
α_{1C}	5′-GGAGCTGGACAAGGCTATGA-3′ 5′-GACCTAGAGAGGCAGAGCGA-3′	653 bp	M67515	[51]
α_{1D}	5′-GACTCAGATTACAACCCAGG-3′ 5′-GTGGTGTTCTTCGCAGGGTA-3′	640 bp	M57682	[19]
α_{1S}	5′-CTGGAAAGGACCAACTCTCT-3′ 5′-TGAGCCGAATTCCTGGGAAC-3′	505 bp	L04684	[56]
α_{1E}	5′-AATATTCCAGTTGGCTTGTAT-3′ 5′-GTAACTTCTGCGTCGTGACT-3′	198 bp	L15453	[52]
α_{1G}	5′-CCAGGTCTCTAGGGCTATAG-3′ 5′-TGTGGGGATCCCGGAGGTTCA-3′	772 bp	AF051947	[40]
α_{1I}	5′-CAGGACCTCAACGCCAGCGG-3′ 5′-GGTCCGAGGAGACCCCATCC-3′	780 bp	AF086827	[24]
β1	5′-AGCATGCCAGTGTGCACGAGTAC-3′ 5′-AGCCCTCCAGCTCATTCTTATTGC-3′	387 bp	X61394	[41]
β2	5′-ATAACCACAGAGAGGAGAGCCAC-3′ 5′-TATACATCCCTGTTCCACTCGCCA-3′	208 bp	M80545	[39]
β3	5′-TCCCTGGACTTCAGAACCAGCAG-3′ 5′-TTGTGGTCATGCTCCGAGTCCTG-3′	280 bp	M88751	[7]
β4	5′-TGAGGCATAGCAACCACTCTACAG-3′ 5′-ATGTCGGGAGTCATGGCTGCATC-3′	241 bp	L02315	[8]

Table 1). For amplification a predenaturation step at 94°C for 1 min was used followed by 40 cycles consisting of three temperature steps (1st step: 94°C; 2nd step: annealing temperature different for each primer pair; 3rd step: 72°C; each temperature step lasted for 1 min) terminated by an elongation step at 72°C for 5 min. The annealing temperature was calculated for every primer pair from the G/C and A/T content of the oligonucleotide primers used in the reaction. Amplified DNA fragments were analyzed by agarose gel electrophoresis and sequenced. The control RNA was extracted from brain and skeletal muscle of a Wistar rat. The tissues were removed after decapitation. RNA extraction from the tissues was performed following the same protocol as with GH_3/B_6 cells.

Measurement of prolactin secretion

Prolactin secretion of GH_3/B_6 cells was measured semiquantitatively with the reverse hemolytic plaque assay (RHPA) [49] following the procedure as described previously [2]. GH_3/B_6 cells were mixed with protein-A-coupled ovine erythrocytes and infused into Cunningham chambers with a volume of about 60 µl. The cells were allowed to settle for about 1 h in a humidified incubator (37°C, 95% air/5% CO_2). Before the cells were kept in culture medium overnight, the unattached cells were removed by washing with Ham's F10+0.1% BSA. For the plaque assay the cells in the Cunningham chambers were rinsed with Ham's F10 and then incubated for 2.5 h in Ham's F10/BSA containing antibody against rat prolactin [1:100, anti-rPRL-IC-5; National Hormone and Pituitary Program (NHPP), Torrance, USA] together with 10 µM nifedipine or 10 nM ω-agatoxin IVA + 200 nM ω-conotoxin MVIIC or 200 µM Cd^{2+} or without any drugs and toxins as control. After the incubation period, guinea pig complement (1:50) was added for 45 min to develop plaques. Afterwards, the cells were fixed with 2% glutaraldehyde in 0.9% NaCl solution. The measurement of plaque areas was made by using the software "NIH Image" by Wayne Rasband (National Institute of Health, USA).

Chemicals

One batch of ω-agatoxin IVA was a kind gift of Dr. Nicholas A. Saccomano (Pfizer, Groton, Conn., USA). Another batch of ω-agatoxin IVA as well as ω-conotoxin VIA and ω-conotoxin MVIIC were purchased from Alamone Labs (Jerusalem, Israel). The toxins were dissolved in distilled water to obtain a stock solution of 100 µM and kept in aliquots at –20°C. For final use the aliquots were diluted with bath solution. Nifedipine (Sigma) was dissolved in DMSO, and the stock solution had a concentration of 10 mM. Before each experiment a solution of the final concentration of nifedipine and/or toxins was prepared and sonicated. Solutions with peptide toxins contained 0.1% BSA to prevent unspecific absorption.

Results

Ca^{2+} channel currents in GH_3/B_6 cells

Ca^{2+} channel currents were recorded with Ba^{2+} as the charge carrier. Na^+ currents were blocked by adding TTX to the external solution and K^+ currents were abolished by using Cs^+ as the principal cation of the pipette solution. As shown in Fig. 1A, Ba^{2+} currents were activated with depolarizing potential steps from a holding potential of –70 mV. These Ba^{2+} currents did not inactivate within the 50-ms pulse duration. There was also only a very slow or even no inactivation of the Ba^{2+} currents when the test pulse was prolonged to 20 s (n=13; data not shown). The voltage dependence of Ba^{2+} currents was also determined with 500-ms voltage-ramp commands from –100 to 80 mV. From a holding potential of –70 mV these ramp pulses activated Ca^{2+} channel currents at –46±4 mV (mean ±SD, n=37) and currents increased to a maximum inward current of 381±367 pA at –8±5 mV. Almost identical Ca^{2+} channel currents were recorded with ramp pulses from a holding potential of –40 mV. In most experiments, there was no indication of Ba^{2+} current activation at more negative potentials than –50 mV. The same result was obtained with ramp pulses of 100 (n=3) or 200 ms (n=3; Fig. 1B). These Ba^{2+} currents were completely blocked by 200 µM Cd^{2+} (n=30) and to about 95% by 3 mM Ni^{2+} (n=4).

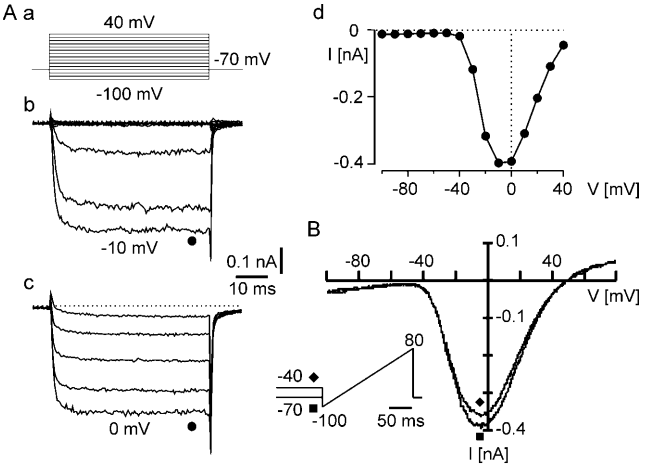

Fig. 1A, B Whole-cell Ba^{2+} currents in GH_3/B_6 cells. **A** From a holding potential of –70 mV Ba^{2+} currents were elicited with 50-ms steps to membrane potentials between –100 and 40 mV in steps of 10 mV as indicated in the pulse diagram (**Aa**). For clarity, in **Ab** current traces recorded at membrane potentials between –100 and –10 mV, in **Ac** those recorded between 0 and 40 mV were superimposed. **Ad** Steady-state current amplitudes of the membrane currents shown in **Ab** and **Ac** (●) plotted against membrane potential. **B** Superimposition of Ba^{2+} currents recorded with 200-ms ramp pulses from –100 to 80 mV starting from two different holding potentials, –70 mV (■) and –40 mV (◆)

From 50 GH_3/B_6 cells tested only 5 cells exhibited T-type Ca^{2+} channel currents of small amplitude (less than 5% of the total Ba^{2+} current amplitude). After treatment with estradiol (1 nM for 3 days) the percentage of cells exhibiting T-type currents increased (7 out of 14 cells) as well as their amplitudes as compared with control cells. The T-type current was activated at membrane potentials more positive than –60 mV and was half-activated at –34.7±0.3 mV (n=6), a membrane potential similar to that found in GH_3 cells (–32 mV [48]). Small T-type current amplitudes have also been reported in GH_3 cells (about 10% [9]) and native gonadotrophs [58]. The presence of the small T-type Ca^{2+} channel currents in untreated cells did not disturb the measurement of HVA Ca^{2+} channel current amplitudes in the experiments performed with a holding potential of –70 mV.

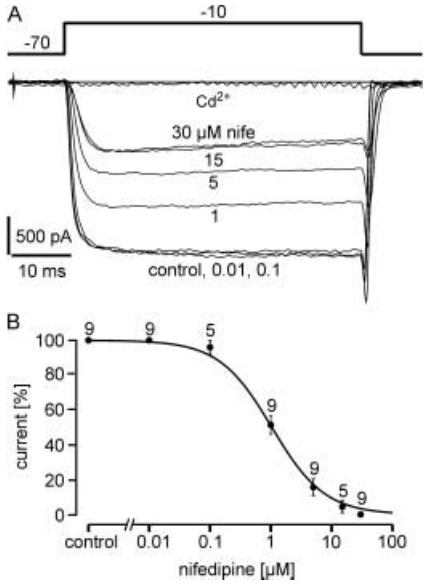

Fig. 2A, B Concentration-dependent reduction of Ba^{2+} currents by nifedipine. **A** Superimposed Ba^{2+} currents elicited with a 50-ms step to –10 mV from a holding potential of –70 mV after sequential application of nifedipine concentrations increasing from 0.01 to 30 µM. The nifedipine-insensitive current was blocked by 200 µM Cd^{2+}. **B** Dose–response curve of nifedipine. The Ba^{2+} current inhibition induced by nifedipine concentrations between 0.01 and 30 µM is given as the percentage of the current inhibition induced by 30 µM nifedipine (mean values ± SEM). The data points were fitted to a sigmoidal function. The calculated IC_{50} value was 1.0 µM. *Numbers* near means denote number of cells studied

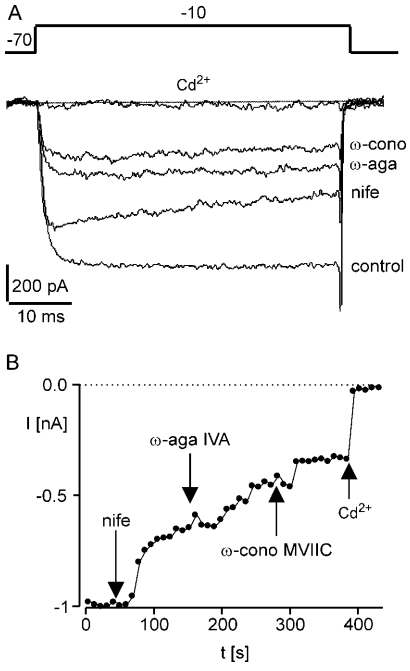

Fig. 3A, B Pharmacological separation of the different Ba^{2+} current subtypes. **A** Ba^{2+} currents recorded with a 50-ms test pulse to –10 mV from a holding potential of –70 mV. Control current and currents recorded after sequential application of nifedipine (5 µM; *nife*), ω-agatoxin IVA (10 nM; *ω-aga*), ω-conotoxin MVIIC (200 nM; *ω-cono*) and Cd^{2+} (200 µM) superimposed. **B** Amplitudes of Ba^{2+} inward currents elicited every 10 s with a constant test pulse plotted against time. *Arrows* indicate times at which drugs and toxins were applied

Pharmacological separation of different Ca^{2+} channel current subtypes

To determine the appropriate nifedipine concentration to separate the DHP-sensitive Ca^{2+} channel current from the other current components, the dose–response relation for nifedipine was measured in GH_3/B_6 cells. Figure 2A shows that increasing concentrations of nifedipine reduced the Ba^{2+} current elicited with test pulses to –10 mV from a holding potential of –70 mV, 15 µM and 30 µM nifedipine were almost equally effective. The current amplitude blocked by 30 µM nifedipine was taken as the total nifedipine-sensitive current to which the current inhibition induced by lower nifedipine concentrations was related. The dose–response curve yielded an IC_{50}=1.0 µM (Fig. 2B). In the following experiments, 5 or 10 µM nifedipine was used, concentrations sufficient to inhibit about 90% of the L-type Ca^{2+} channel current and low enough to prevent blockage of other Ca^{2+} channel subtypes.

The experiment of Fig. 2A demonstrates the existence of a nifedipine-insensitive Ca^{2+} channel current in GH_3/B_6 cells which could totally be blocked by Cd^{2+}. Figure 3 shows that this remaining current consisted of several components which were isolated by different toxins. A test potential to –10 mV was applied from a holding potential of –70 mV every 10 or 15 s. After application of nifedipine (10 µM) a steady-state block of the Ba^{2+} current was achieved within about 2 min (Fig. 3B). In the presence of nifedipine the unblocked current slowly decayed (Fig. 3A) presumably due to the voltage-dependent block of nifedipine [16]. Thereafter, ω-agatoxin IVA (10 nM) [33] and ω-conotoxin MVIIC (200 nM) [59] were applied. Each of these toxins was able to induce an additional steady-state block of the Ba^{2+} current, suggesting that in addition to nifedipine-sensitive Ca^{2+} channel currents (L-type) there are also P- and Q-type Ca^{2+} channel currents in GH_3/B_6 cells. The presence of a Q-type current is also demonstrated in Fig. 4C. At the end of the experiment the toxin-resistant current was totally blocked by Cd^{2+} (200 µM).

The amount of current inhibition induced by nifedipine and a high concentration of ω-agatoxin IVA (1 µM) was dependent on the sequence of drug or toxin application. If nifedipine (10 µM) was applied first, then the control current was reduced by about 50% (53±6%, *n*=7; mean ± SEM). If the P/Q-type Ca^{2+} channel blocker ω-agatoxin IVA (1 µM) was applied first, then the current was also reduced by about 50% (49±11%, *n*=4). However, after pretreatment of GH_3/B_6 cells with nifedipine, ω-agatoxin IVA blocked only about half of the nifedipine-resistant current, i.e., about 25% of the control current (Fig. 4A). A similar result was obtained when nifedipine was applied after application of 1 µM ω-agatoxin IVA (Fig. 4B). In both cases the drug-resistant cur-

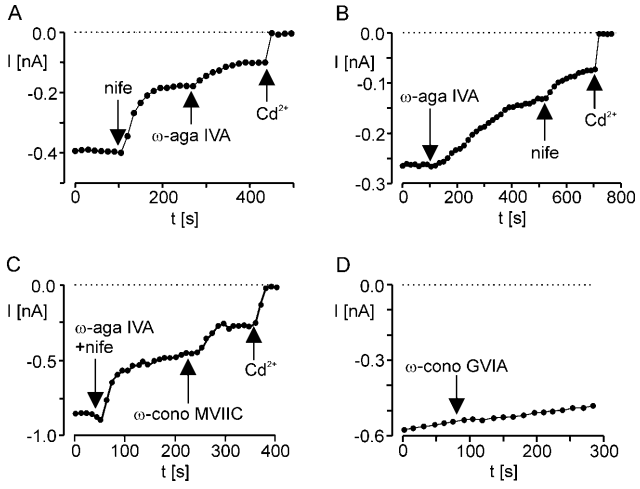

Fig. 4A–D Separation of different subtypes of Ba^{2+} currents. In each *panel* an experiment on a different GH_3/B_6 cell is shown. Maximum inward current amplitudes of Ba^{2+} currents recorded with a constant test pulse to –10 mV from a holding potential of –70 mV applied every 15 s (**A**, **B**, **D**) or 10 s (**C**) plotted against time. **A** Application of nifedipine (10 µM) followed by application of ω-agatoxin IVA (1 µM) and Cd^{2+} (200 µM). **B** Application of ω-agatoxin IVA (1 µM) followed by application of nifedipine (10 µM) and Cd^{2+} (200 µM). **C** Application of ω-agatoxin IVA (10 nM) together with nifedipine (10 µM) followed by application of ω-conotoxin MVIIC (200 nM) and Cd^{2+} (200 µM). **D** Application of ω-conotoxin GVIA (2 µM)

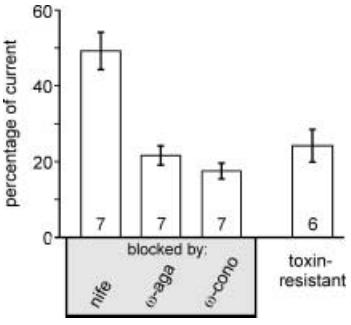

Fig. 5 Percentage of current inhibition by nifedipine and the peptide toxins as well as the percentage of the toxin-resistant current in relation to the total Ba^{2+} current amplitude (mean ± SEM). Currents blocked by 10 µM nifedipine (*nife*), 10 nM ω-agatoxin IVA (*ω-aga*) and 200 nM ω-conotoxin MVIIC (*ω-cono*) were evaluated. Toxin-resistant current denotes the percentage of current remaining unblocked in the presence of 10 µM nifedipine + 10 nM ω-agatoxin IVA + 200 nM ω-conotoxin MVIIC. *Numbers* within the *columns* give the number of experiments evaluated

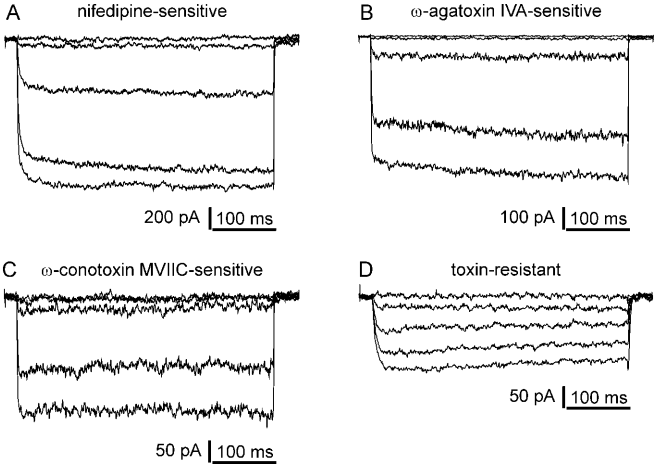

Fig. 6A–D Pharmacological separation of different Ca^{2+} channel currents in GH_3/B_6 cells. Nifedipine- (**A**), ω-agatoxin-IVA- (**B**) and ω-conotoxin-MVIIC-sensitive currents (**C**) were obtained by subtracting the current traces recorded in the presence of the substance or toxin from the corresponding control current traces. **D** The toxin-resistant current was recorded in the presence of nifedipine (10 µM), ω-agatoxin IVA (10 nM) and ω-conotoxin MVIIC (200 nM). The holding potential was –50 mV (**A**–**C**) or –40 mV (**D**) and currents were elicited with test pulses from –50 mV to –10 mV (**A**–**C**) or –40 mV to 0 (**D**) in 10-mV increments

rents were blocked completely by 200 µM Cd^{2+}. This group of experiments indicated that the high concentration of ω-agatoxin IVA (1 µM) presumably blocked part of the L-type Ca^{2+} channels, similarly as has been shown for cerebellar granule neurons [38]. Therefore, the further analysis was performed using ω-agatoxin IVA at the low concentration of 10 nM to selectively block P-type channels [6]. To block Q-type channels 200 nM ω-conotoxin MVIIC was employed. Nifedipine was used at concentrations of 5 or 10 µM, which are close to a saturating concentration. The amplitude of the nifedipine-sensitive Ca^{2+} channel current (Fig. 2) was taken as the L-type Ca^{2+} channel current amplitude [29]. The N-type Ca^{2+} channel blocker ω-conotoxin GVIA (2 µM) had no effect on Ca^{2+} channel currents (n=6; Fig. 4D), indicating that N-type Ca^{2+} channels do not exist in GH_3/B_6 cells. To determine the mean contribution of a particular Ca^{2+} channel current subtype to the total Ba^{2+} current, the current inhibition induced by nifedipine or one of the toxins was studied. Figure 5 summarizes the results: 10 µM nifedipine inhibited the Ba^{2+} current by 49.1±4.9% (L-type), 10 nM ω-agatoxin IVA by 21.6±2.5% (P-type) and 200 nM ω-conotoxin MVIIC by 17.5±2.1% (Q-type). The toxin-resistant current amounted to 24.1±4.3%. Application of 5 µM nifedipine reduced the Ba^{2+} current by 45.8±3.1% (n=13). The fact that the sum of all current components exceeds 100% shows that nifedipine and the toxins are not strictly selective in blocking the different Ca^{2+} channels.

Ca^{2+} channel current subtypes

Subtraction of the current traces elicited in the presence of 10 µM nifedipine from the control currents yielded the nifedipine-sensitive current (Fig. 6A). P- and Q-type Ca^{2+} channel currents were obtained as the ω-agatoxin-IVA-sensitive (10 nM) and ω-conotoxin-MVIIC-sensitive (200 nM) currents, respectively (Fig. 6B, C). The toxin-resistant Ca^{2+} channel currents were the Ba^{2+} currents recorded in the presence of 10 µM nifedipine, 10 nM ω-agatoxin IVA and 200 nM ω-conotoxin MVIIC (Fig. 6D). Figure 6 shows membrane currents recorded from a hold-

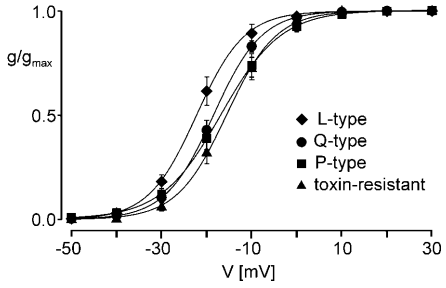

Fig. 7 Activation curves of L-, P-, Q-type and toxin-resistant Ca^{2+} channel currents. Conductances were calculated from the current amplitudes of the nifedipine-sensitive current (L-type), 10 nM ω-agatoxin-sensitive current (P-type), ω-conotoxin-MVIIC-sensitive current (Q-type) and toxin-resistant Ba^{2+} current, assuming a Ba^{2+} current reversal potential of 40 mV. Conductances were normalized to the maximal conductance and their relation to the test pulse potential fitted to Boltzmann functions. Shown are mean Boltzmann functions yielding: L-type ($V_{1/2}$=–22.3 mV, k=5.3 mV; n=6), Q-type ($V_{1/2}$=–18.4 mV, k=5.3 mV; n=6), P-type ($V_{1/2}$=–17.3 mV, k=6.0 mV; n=5), toxin-resistant ($V_{1/2}$=–15.6 mV, k=5.5 mV; n=8). $V_{1/2}$ denotes the membrane potential at which half of the Ca^{2+} channel current is activated and k (mV) denotes the slope of the curve

ing potential of –50 mV (A–C) or –40 mV (D). Similar measurements were performed from a holding potential of –70 mV (not shown). The time constant for L-type current activation at –10 mV was 1.7±0.3 ms (n=6), whereas current activation of P- and Q-type currents at –10 mV was very fast with time constants of less than 1 ms. As shown in Fig. 6 the time course of current activation of the toxin-resistant current at –10 mV was slower than that of the other currents (τ=5.1±0.7 ms; n=8).

To determine the voltage dependence of the different Ba^{2+} current components, the conductances were calculated from the peak or steady-state inward currents, normalized to the maximum conductance and plotted against membrane potential (Fig. 7). The membrane potential for 50% activation of the different Ca^{2+} channel currents ($V_{1/2}$) and the slope of the activation curves (k) for each current subtype were: L-type ($V_{1/2}$=–22.3±0.2 mV; k=5.3±0.2 mV; n=6), Q-type ($V_{1/2}$=–18.4±0.1 mV; k=5.3±0.1 mV; n=4), P-type ($V_{1/2}$=–17.3±0.1 mV; k=6.0±0.1 mV; n=5), toxin-resistant ($V_{1/2}$=–15.6±0.2 mV; k=5.5±0.2 mV; n=8). The experiments performed to determine the time and voltage dependence of Ca^{2+} channel current activation were recorded from a holding potential of –50 mV or –40 mV.

Different Ca^{2+} channel α_1 and β subunits are expressed in GH_3/B_6 cells

RT-PCR was performed to study the expression of α_1 and β Ca^{2+} channel subunits. These results are summarized in Fig. 8. The presence of the α_{1G} subunit mRNA may indicate that this subunit is the molecular correlate of the T-type Ca^{2+} channel, whereas transcripts for α_{1I}, another T-type Ca^{2+} channel α_1 subunit, were not found. The third α_1 subunit (α_{1H}), which is thought to be a pore-forming subunit for T-type Ca^{2+} channels [42], was not studied, because it has not yet been cloned from the rat. All known L-type Ca^{2+} channel α_1 subunit mRNAs (α_{1C}, α_{1D}, and α_{1S}) are expressed in GH_3/B_6 cells. This is astonishing, because α_{1S} has so far been shown to be expressed almost exclusively in skeletal muscle [54]. In accordance with the electrophysiological data, the transcripts for the α_{1A} subunit that may take part in the formation of P/Q-type Ca^{2+} channels was present in GH_3/B_6 cells, whereas the mRNA for the α_{1B} subunit, which has been shown to form the N-type Ca^{2+} channel [54], was not found in GH_3/B_6 cells. The absence of transcripts for the α_{1E} subunit and the presence of a toxin-resistant Ca^{2+} channel suggests that the toxin-resistant current in GH_3/B_6 cells is not mediated by R-type Ca^{2+} channels. In addition, mRNAs for the β1–3 subunits are expressed in GH_3/B_6 cells, whereas transcripts for the β4 subunit were not found. A summary of the pharmacological and RT-PCR results is given in Table 2.

Blockage of L- or P/Q-type Ca^{2+} channels decreases cell excitability

Current-clamp experiments were performed using 22 GH_3/B_6 cells. Ten cells were silent and 12 cells spontaneously fired action potentials. The action potentials had a peak potential of –12.2±2.8 mV, a threshold potential

Table 2 Ca^{2+} channel α_1 subunits and their assumed electrophysiological correlates in GH_3/B_6 cells. Transcripts for α_{1B} and α_{1E} were not found. (*n.d.* Not determined)

Subunit	mRNA	Subtype	Test substance	Ba^{2+} current
α_{1C}	+	L	Nifedipine (10 μM)	+
α_{1D}	+			
α_{1S}	+			
α_{1A}	+	P	ω-Agatoxin (10 nM)	+
		Q	ω-Conotoxin MVIIC (200 nM)	+
?		Toxin-resistant	Cd^{2+} (200 μM) in the presence of nifedipine (10 μM) + ω-agatoxin (10 nM) + ω-conotoxin MVIIC (200 nM)	+
α_{1G}	+	T	–	+
α_{1H}	n.d.			
α_{1I}	–			

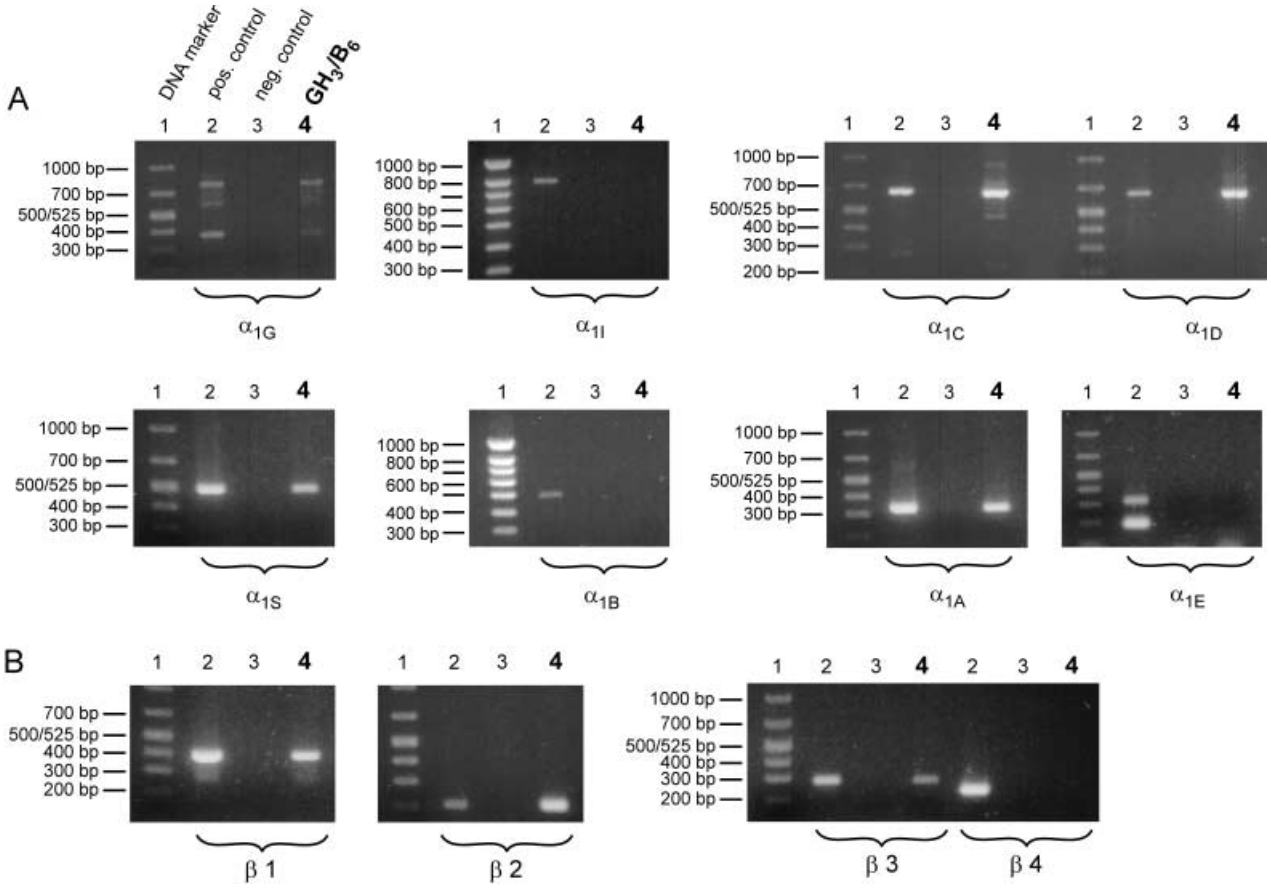

Fig. 8A, B Transcripts for Ca^{2+} channel α_1 (**A**) and β (**B**) subunits present in GH_3/B_6 cells. RT-PCRs performed as described in Materials and methods. Ten percent of the PCR products were separated on a 1.5% agarose gel. *Lane 1*, DNA marker; *lane 2*, positive control. For all α_1 and β subunits brain cDNA was used as a positive control, except for α_{1S} where cDNA from skeletal muscle was used. *Lane 3*, negative control (H_2O); *lane 4*, cDNA from GH_3/B_6 cells. In the α_{1I} panel the 700-bp DNA fragment and in the α_{1B} panel the 500- and 700-bp DNA fragments are not indicated

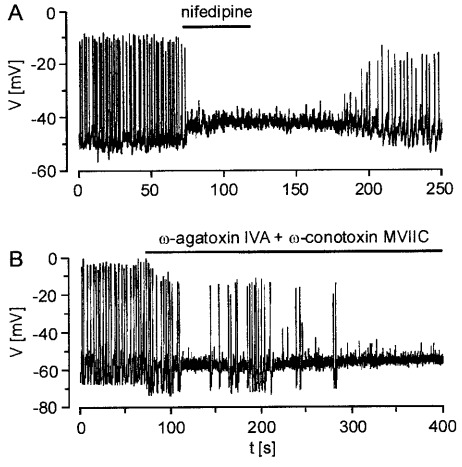

Fig. 9A, B Blockage of L-type (**A**) or P/Q-type Ca^{2+} channels (**B**) inhibits action potential firing. The measurement of membrane potentials was performed with the perforated-patch whole-cell configuration. *Bars* indicate the times for which nifedipine (10 μM) in **A** or the toxins (10 nM ω-agatoxin IVA + 200 nM ω-conotoxin MVIIC) in **B** were applied

of –45.1±1.1 mV and an afterhyperpolarizing potential of –59.6±2.2 mV. The mean action potential duration measured at the threshold potential was 135±76 ms and the mean firing frequency was 0.41±0.05 Hz. These parameters are similar to those reported for GH_3 cells [45]. In silent cells application of 10 μM nifedipine induced a small depolarization from –45±2 mV to –41±2 mV (n=8), in firing cells the spontaneous generation of action potentials was abolished (n=4; Fig. 9A). Application of 10 nM ω-agatoxin IVA + 200 nM ω-conotoxin MVIIC induced no change in the resting membrane potential (–50±2 mV; n=4), but blocked the firing of spontaneous action potentials (n=8; Fig. 9B).

Blockage of L- and P/Q-type Ca^{2+} channels decreases prolactin secretion

Prolactin secretion from GH_3/B_6 cells was measured semiquantitatively with RHPA [2, 49]. The time course of plaque formation has previously been shown to reach a steady state within about 4 h [4]. We used a shorter incubation time (2.5 h) to improve conditions for detecting the changes in prolactin secretion induced by the drugs and peptide toxins. The numbers of cells evaluated were: 5407 (control), 2555 (nifedipine) and 4569 (peptide tox-

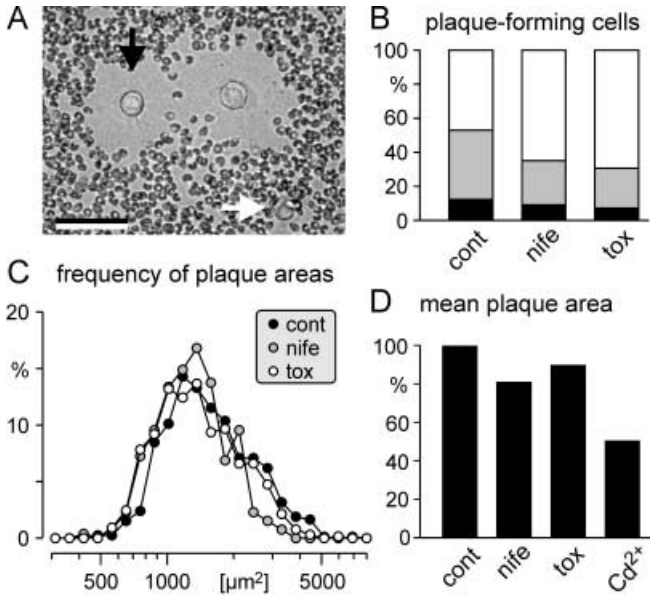

Fig. 10A–D Measurement of prolactin secretion from GH_3/B_6 cells performed with the reverse hemolytic plaque assay (*RHPA*). **A** Micrograph with two plaques each containing a single secreting GH_3/B_6 cell (*black arrow*) as well as a non-secreting cell (*white arrow*). *Scale bar* denotes 50 µm. **B** Percentages of non-secreting cells (*white*), cells located in multi-cell plaques (*gray*) and single-cell plaques (*black*) under control conditions (*cont*), in the presence of 10 µM nifedipine (*nife*) and 10 nM ω-agatoxin IVA + 200 nM ω-conotoxin MVIIC (*tox*). **C** Normalized frequency distribution of single-cell plaque areas of GH_3/B_6 cells under control condition (*black symbol*), in the presence of nifedipine (*gray symbol*) and peptide toxins (*white symbol*). **D** Mean plaque areas obtained in the control condition (*cont*), in the presence of nifedipine (*nife*), peptide toxins (*tox*) and 200 µM Cd^{2+}

ins). Under control conditions 53% of the cells were found within plaques. There were two types of plaques: one type contained only one cell in the center of a plaque (12% of the total cell number in the control) as shown in Fig. 10A, the other type contained two to seven cells (multi-cell plaques; 41% of the total cell number). In the case of the multi-cell plaques it was not possible to determine how many of the cells contributed to the plaque formation. The number of cells within plaques decreased to 35% in the presence of 10 µM nifedipine (26% in multi-cell plaques, 9% in single-cell plaques) and to 30% (23% in multi-cell plaques, 7% in single-cell plaques; Fig. 10B) in the presence of 10 nM ω-agatoxin IVA + 200 nM ω-conotoxin MVIIC. The mean number of cells in the multi-cell plaques was independent of the condition under investigation: 2.6 (control), 2.6 (nifedipine), and 2.7 (peptide toxins). To determine the influence of the different conditions on prolactin secretion in addition to the percentage of plaque-forming cells the plaque areas were evaluated. To obtain unequivocal results we determined the areas of the single-cell plaques only. The frequency distribution of these areas determined under the different conditions are plotted in Fig. 10C. The mean plaque areas were 1818±32 µm² (control; mean ± SEM; n=791), 1468±33 µm² (nifedipine; n=262), and 1628±30 µm² (peptide toxins; n=652). In the presence of 200 µM Cd^{2+} only 20 cells out of several thousand cells (not exactly determined) formed plaques, the mean area was 914±79 µm². The "secretion index", as calculated by the percentage of plaque-forming cells multiplied by the mean plaque area, showed that basal prolactin secretion in the presence of nifedipine decreased to about 60% and in the presence of the peptide toxins to about 52% of the control. In the presence of Cd^{2+} the secretion index decreased to a value far below 1%.

Discussion

In GH_3/B_6 cells five different Ca^{2+} channel currents can be distinguished: T-, L-, P-, Q-type and toxin-resistant. About 50% of the Ca^{2+} channel current amplitude is mediated by L-type current, the remaining current is mediated by P/Q-type and toxin-resistant Ca^{2+} channels. The T-type current amplitude is negligible in GH_3/B_6cells. Although the relative amplitudes vary, the same Ca^{2+} current subtypes have been found in corticotrophs [21], clonal murine corticotroph AtT-20 cells [26], and melanotrophs [12]. The presence of N-type Ca^{2+} channels, which are ubiquitous in the brain [54], has not reported in most studies investigating clonal and native pituitary cells. However, there is one study of GH_3 cells in which a tiny percentage (≅4%) of the Ca^{2+} current is mediated by ω-conotoxin-GVIA-sensitive N-type-like Ca^{2+} channels [60].

L-type Ca^{2+} channel current

L-type Ca^{2+} currents are characterized by slowly inactivating or non-inactivating currents which are blocked by DHPs (reviewed in [36]). From a holding potential of –70 mV, the IC_{50} for nifedipine in GH_3/B_6 cells was 1 µM, in agreement with an IC_{50}=1 µM for nitrendipine in GH_3 cells [48]. Decreasing the holding potential from –80 mV to –32 mV, the IC_{50} decreased to 10 nM, demonstrating the strong potential dependence of the DHP-induced block of L-type channels [48].

Fifty percent of the nifedipine-sensitive L-type current in GH_3/B_6 cells was activated at –22 mV, i.e., at a more negative membrane potential than that reported for HVA currents in GH_3 cells (–14 mV) [13] and gonadotrophs (–13 mV) [55] and for L-type currents in corticotrophs (–12 mV) [21]. However, there are other reports of DHP-sensitive currents in GH_3 cells activating at relatively negative membrane potentials. If the nifedipine-sensitive L-type current was elicited from a holding potential of –90 mV, it was reported to have a maximum inward current near –35 mV [9]. In addition, GH_3 cells possess a DHP-sensitive steady-state Ca^{2+} current, which activates at membrane potentials positive to –50 mV and peaks at about –30 mV [46]. These observations indicate that the L-type current in GH_3 and possibly also in GH_3/B_6 cells may be composed of at least two different

L-type currents, with one component already activated at the resting membrane potential [28].

P-type and Q-type Ca^{2+} channel currents

The relative amplitude of the DHP-insensitive current in GH_3 cells has been reported to vary between 50% [1], 20% [9] and very small values of the total Ca^{2+} channel current [20, 25, 48]. We found that in GH_3/B_6 cells about 50% of the Ba^{2+} current was insensitive to nifedipine and consisted of at least three different Ba^{2+} current components. In corticotrophs a P-type but not a Q-type current was described [21], and in melanotrophs P- and Q-type Ca^{2+} currents were observed [12]. Generally, the presence of physically different populations of P- and Q-type channels is assumed if part of the Ca^{2+} current can selectively be blocked by a selective toxin [37, 54]. In GH_3/B_6 cells we could distinguish P- and Q-type currents with the help of different toxins, but their biophysical properties are too similar to perform a successful electrophysiological separation.

Toxin-resistant Ca^{2+} channel current

In GH_3/B_6 cells the toxin-resistant Ca^{2+} current comprises 24% of the total Ca^{2+} current and its voltage dependence of current activation is similar to that of P- and Q-type currents. Toxin-resistant Ca^{2+} currents were also described in corticotrophs [21], melanotrophs [12], and AtT-20 cells [26]. The toxin-resistant current in GH_3/B_6 cells activated with a slower time course than P- and Q-type currents and did not inactivate, similar to the toxin-resistant current in corticotrophs [21]. In contrast, the toxin-resistant R-type Ca^{2+} current described in neurons is an inactivating current [43] and the ionic channels mediating this current are assumed to be formed by α_{1E} subunits [57]. The notion that the toxin-resistant current in GH_3/B_6 cells is not mediated by R-type channels is further supported by the absence of transcripts for α_{1E} subunits in these cells.

Molecular correlates of the different Ca^{2+} channel subtypes

Ca^{2+} channels are heteromultimers consisting of a pore-forming α_1 subunit and different combinations of auxiliary subunits (α_2, δ, β, γ). The α_1 subunits so far cloned presumably mediate the T-type (α_{1G}, α_{1H}, α_{1I}), L-type (α_{1C}, α_{1D}, α_{1S}), P/Q-type (α_{1A}) and R-type channel (α_{1E}), reviewed in [42, 54]. Previous studies have shown that in the pituitary and GH subclones (GH_4/C_1, GH_3) α_{1A}, α_{1C} and α_{1D} are expressed [25, 50]. This is also true for GH_3/B_6 cells. In addition these cells express two other α_1 subunits (α_{1S}, α_{1G}) and three of the four cloned β subunits (β_{1-3}). A possible candidate for the pore-forming subunit of the T-type channel in GH_3/B_6 cells is α_{1G}. Transcripts for α_{1I} were not found and the expression of α_{1H} was not studied because the rat homologue of the human subunit has not been cloned, as pointed out above. In GH_3/B_6 cells the transcripts for all pore-forming α_1 subunits of L-type channels (α_{1C}, α_{1D}, α_{1S} [54]) were found. It is not known which of these subunits contribute to the nifedipine-sensitive current. Due to their different sensitivities to ω-agatoxin IVA and ω-conotoxin MVIIC, P- and Q-type Ca^{2+} channel currents were distinguished in GH_3/B_6 cells. The likely candidate for the molecular correlate for both channels is the α_{1A} subunit. As yet it is not known whether P- and Q-type channels are formed by different splice variants of the α_{1A} subunit [5] or by the same α_{1A} subunit associated with different auxiliary subunits [3, 31, 42]. The molecular correlate for the channels mediating the toxin-resistant current in GH_3/B_6 cells is not known. Transcripts for α_{1E} presumably mediating the R-type current in cerebellar granule cells [43] were not found in GH_3/B_6 cells.

In GH_3/B_6 cells three β subunit genes ($\beta1$–$\beta3$) are expressed. Coexpression of β subunits with α_1 subunits in heterologous expression systems increased the current density and shifted the voltage dependence of activation and inactivation curves towards more negative membrane potentials [3, 54]. Therefore, it is possible that β subunits are involved in shifting the voltage dependence of L-type currents to more negative membrane potentials in GH_3/B_6 cells.

Function of the different Ca^{2+} channel subtypes

The secretion of prolactin and growth hormone from GH_3/B_6 cells is controlled by the $[Ca^{2+}]_i$ which is mainly determined by influx of Ca^{2+} through the different voltage-dependent Ca^{2+} channel subtypes [14]. Blockage of L-type Ca^{2+} channels by nifedipine totally blocked the firing of spontaneous action potentials in GH_3/B_6 cells. Spontaneous activity was also blocked in the presence of the peptide toxins inhibiting P/Q-type Ca^{2+} channels. The secretion index, which mirrors prolactin secretion, was reduced to about 60% by nifedipine blocking L-type channels and to about 52% by the peptide toxins blocking P/Q-type channels. These results may reflect the fact that part of basal prolactin secretion depends on Ca^{2+} influx during the spontaneous firing of action potentials. Blockage of all Ca^{2+} channels with Cd^{2+} decreased the secretion index to less than 1%, indicating that basal prolactin secretion depends on the activation of voltage-dependent Ca^{2+} channels near the resting potential and do not require the firing of action potentials [35]. Ca^{2+} influx through L-type channels seems to be the main source for the increase in $[Ca^{2+}]_i$ during an action potential [34]. Several reports have demonstrated that blocking L-type channels abolishes the oscillations of $[Ca^{2+}]_i$ elicited by the spontaneous firing of action potentials [10, 47]. A similar role of L-type channels for $[Ca^{2+}]_i$ in spontaneously spiking cells has been demonstrated in

corticotrophs [22]. Abolition of Ca^{2+} oscillations in GH_3 cells by 10 µM nimodipine reduced spontaneous prolactin secretion by 33% [10], a value similar to that reported in this study. However, in AtT-20 cells total blockage of L-type channels induced a much larger inhibition of ACTH release, comparable to that induced by Cd^{2+} [26]. In GH_3/B_6 cells the inhibition of P/Q-type Ca^{2+} channels also abolished the firing of spontaneous action potentials and decreased prolactin secretion to about 52% of the control value. In contrast, blockage of P/Q-type channels in clonal AtT-20 cells had no significant effect on secretion [26], whereas the inhibition of P/Q-type channels by activation of heterologously expressed D3 receptors in AtT-20 cells decreased ACTH secretion considerably [23]. Ca^{2+} influx through P/Q-type Ca^{2+} channels in melanotrophs is coupled with the same efficiency to exocytosis as the other Ca^{2+} channel subtypes [27]. These data show that the different Ca^{2+} channel subtypes may have different functions in different cell types. Therefore, further experiments have to be performed to relate membrane excitability, $[Ca^{2+}]_i$ and release of prolactin and growth hormone to the different Ca^{2+} channel subtypes in GH_3/B_6 and other neuroendocrine cells.

Acknowledgements We thank Dorrit Schiemann for help with the RT-PCR and performing the RHPA. M.H. is a scholar of the DFG Graduiertenkolleg "Neurale Signaltransduktion und deren pathologische Störungen" (GRK 255). The antibody against rat prolactin was a kind gift of Dr. A.F. Parlow, NHPP, Torrance, California, USA.

References

1. Barros F, del Camino D, Pardo LA, de la Peña P (1996) Caffeine enhancement of electrical activity through direct blockade of inward rectifying K^+ currents in GH_3 rat anterior pituitary cells. Pflügers Arch 431:443–451
2. Bauer CK, Schäfer R, Schiemann D, Reid G, Hanganu I, Schwarz JR (1999) A functional role of the erg-like inward-rectifying K^+ current in prolactin secretion from rat lactotrophs. Mol Cell Endocrinol 148:37–45
3. Birnbaumer L, Qin N, Olcese R, Tareilus E, Platano D, Costantin J, Stefani E (1998) Structures and functions of calcium channel beta subunits. J Bioenerg Biomembr 30:357–375
4. Boockfor FR, Schwarz LK (1988) Cultures of GH_3 cells contain both single and dual hormone secretors. Endocrinology 122:762–764
5. Bourinet E, Soong TW, Sutton K, Slaymaker S, Mathews E, Monteil A, Zamponi GW, Nargeot J, Snutch TP (1999) Splicing of α_{1A} subunit gene generates phenotypic variants of P- and Q-type calcium channels. Nature Neurosci 2:407–415
6. Burley JR, Dolphin AC (2000) Overlapping selectivity of neurotoxin and dihydropyridine calcium channel blockers in cerebellar granule neurons. Neuropharmacology 39:1740–1755
7. Castellano A, Wei X, Birnbaumer L, Perez-Reyes E (1993) Cloning and expression of a third calcium channel beta subunit. J Biol Chem 268:3450–3455
8. Castellano A, Wei X, Birnbaumer L, Perez-Reyes E (1993) Cloning and expression of a neuronal calcium channel beta subunit. J Biol Chem 268:12359–12366
9. Cataldi M, Taglialatela M, Guerriero S, Amoroso S, Lombardi G, di Renzo G, Annunziato L (1996) Protein-tyrosine kinases activate while protein-tyrosine phosphatases inhibit L-type calcium channel activity in pituitary GH_3 cells. J Biol Chem 271:9441–9446
10. Charles AC, Piros ET, Evans CJ, Hales TG (1999) L-type Ca^{2+} channels and K^+ channels specifically modulate the frequency and amplitude of spontaneous Ca^{2+} oscillations and have distinct roles in prolactin release in GH_3 cells. J Biol Chem 274: 7508–7515
11. Chomczynski P, Sacchi N (1987) Single-step method of RNA isolation by acid guanidinium thiocyanate-phenol-chloroform extraction. Anal Biochem 162:156–159
12. Ciranna L, Feltz P, Schlichter R (1996) Selective inhibition of high voltage-activated L-type and Q-type Ca^{2+} currents by serotonin in rat melanotrophs. J Physiol (Lond) 490:595–609
13. Cohen CJ, McCarthy RT (1987) Nimodipine block of calcium channels in rat anterior pituitary cells. J Physiol (Lond) 387: 195–226
14. Corrette BJ, Bauer CK, Schwarz JR (1995) Electrophysiology of anterior pituitary cells. In: Scherübl H, Hescheler J (eds) The electrophysiology of neuroendocrine cells. CRC, Boca Raton, Fla., pp 101–143
15. Dubel SJ, Starr TVB, Hell J, Ahlijanian MK, Enyeart JJ, Catterall WA, Snutch TP (1992) Molecular cloning of the alpha-1 subunit of an omega-conotoxin-sensitive calcium channel. Proc Natl Acad Sci USA 89:5058–5062
16. Eliot LS, Johnston D (1994) Multiple components of calcium current in acutely dissociated dentate gyrus granule neurons. J Neurophysiol 72:762–777
17. Hamill OP, Marty A, Neher E, Sakmann B, Sigworth FJ (1981) Improved patch-clamp techniques for high-resolution current recording from cells and cell-free patches. Pflügers Arch 391:85–100
18. Horn R, Marty A (1988) Muscarinic activation of ionic currents measured by a new whole-cell recording method. J Gen Physiol 92:145–159
19. Hui AS, Ellinor PT, Wang J, Schartz A (1991) Molecular cloning of multiple subtypes of a novel rat brain isoform of the alpha-1 subunit of the voltage dependent calcium channel. Neuron 7:35–44
20. Kramer RH, Kaczmarek LK, Levitan S (1991) Neuropeptide inhibition of voltage-gated calcium channels mediated by mobilization of intracellular calcium. Neuron 6:557–563
21. Kuryshev YA, Childs GV, Ritchie AK (1995) Three high threshold calcium channel subtypes in rat corticotropes. Endocrinology 136:3916–3924
22. Kuryshev YA, Childs GV, Ritchie AK (1996) Corticotropin-releasing hormone stimulates Ca^{2+} entry through L- and P-type Ca^{2+} channels in rat corticotropes. Endocrinology 137:2269–2277
23. Kuzhikandathil E, Oxford GS (1999) Activation of human D3 dopamine receptor inhibits P/Q-type calcium channels and secretory activity in AtT-20 cells. J Neurosci 19:1698–1707
24. Lee JH, Daut AN, Cribbs LL, Lacerda AE, Pereverzev A, Klockner U, Schneider T, Perez-Reyes E (1999) Cloning and expression of a novel member of the low voltage-activated T-type calcium channel family. J Neurosci 19:1912–1921
25. Liévano A, Bolden A, Horn R (1994) Calcium channels in excitable cells: divergent genotypic and phenotypic expression of α_1-subunits. Am J Physiol 36:C411–C424
26. Loechner KJ, Kream RM, Dunlap K (1996) Calcium currents in a pituitary cell line (AtT-20): differential roles in stimulus-secretion coupling. Endocrinology 137:1429–1437
27. Mansfelder HD, Kits KS (2000) All classes of calcium channel couple with equal efficiency to exocytosis in rat melanotrophs, inducing linear stimulus-secretion coupling. J Physiol (Lond) 526:327–339
28. Mantegazza M, Fasolato C, Hescheler J, Pietrobon D (1995) Stimulation of single L-type calcium channels in rat pituitary GH3 cells by thyrotropin-releasing hormone. EMBO J 14: 1075–1083
29. Marchetti C, Amico C, Usai C (1995) Functional characterization of the effect of nimodipine on the calcium current in rat cerebellar granule cells. J Neurophysiol 73:1169–1180
30. Matteson DR, Armstrong CM (1986) Properties of two types of calcium channels in clonal pituitary cells. J Gen Physiol 87: 161–182

31. Mermelstein PG, Foehring RC, Tkatch T, Song WJ, Baranauskas G, Surmeier DJ (1999) Properties of Q-type calcium channels in neostriatal and cortical neurons are correlated with β subunit expression. J Neurosci 19:7268–7277
32. Meza U, Avila G, Felix R, Gomora JC, Cota G (1994) Long-term regulation of calcium channels in clonal pituitary cells by epidermal growth factor, insulin, and glucocorticoids. J Gen Physiol 104:1019–1038
33. Mintz IM, Adams ME, Bean BP (1992) P-type calcium channels in rat central and peripheral neurons. Neuron 9:85–95
34. Mollard P, Schlegel W (1996) Why are endocrine pituitary cells excitable? Trends Endocrinol Metab 7:361–365
35. Mollard P, Theler JM, Guérineau N, Vacher P, Chiavaroli C, Schlegel W (1994) Cytosolic Ca^{2+} of excitable pituitary cells at resting potentials is controlled by steady state Ca^{2+} currents sensitive to dihydropyridines. J Biol Chem 269:25158–25164
36. Mori Y, Mikala G, Varadi G, Kobayashi T, Koch S, Wakamori M, Schwartz A (1996) Molecular pharmacology of voltage-dependent calcium channels. Jpn J Pharmacol 72:83–109
37. Olivera BM, Miljanich GP, Ramachandran J, Adams ME (1994) Calcium channel diversity and neurotransmitter release: the ω-conotoxins and ω-agatoxins. Annu Rev Biochem 63:823–867
38. Pearson HA, Sutton KG, Scott RH, Dolphin AC (1995) Characterization of Ca^{2+} channel currents in cultured rat cerebellar granule neurones. J Physiol (Lond) 482:493–509
39. Perez-Reyes E, Castellano A, Kim HS, Baggstrom E, Lacerda AE, Wei X, Birnbaumer L (1992) Cloning and expression of a cardiac/brain beta subunit of the L-type calcium channel. J Biol Chem 267:1792–1797
40. Perez-Reyes E, Cribbs LL, Daud A, Lacerda AE, Barclay J, Williamson MP, Fox M, Rees M, Lee JH (1998) Molecular characterization of a neuronal low-voltage-activated T-type calcium channel. Nature 391:896–900
41. Pragnell M, Sakamoto J, Jay SD, Campbell KP (1991) Cloning and tissue-specific expression of the brain calcium channel beta-subunit. FEBS Lett 291:253–258
42. Randall A, Benham CD (1999) Recent advances in the molecular understanding of voltage-gated Ca^{2+} channels. Mol Cell Neurosci 14:255–272
43. Randall AD, Tsien RW (1997) Contrasting biophysical and pharmacological properties of T-type and R-type calcium channels. Neuropharmacology 36:879–893
44. Ritchie AK (1993) Estrogen increases low voltage-activated calcium current density in GH_3 anterior pituitary cells. Endocrinology 132:1621–1629
45. Sankaranarayanan S, Simasko SM (1998) Potassium channel blockers have minimal effect on repolarization of spontaneous action potentials in rat pituitary lactotropes. Neuroendocrinology 68:297–311
46. Scherübl H, Hescheler J (1991) Steady-state currents through voltage-dependent, dihydropyridine-sensitive Ca^{2+} channels in GH_3 pituitary cells. Proc R Soc Lond B 245:127–131
47. Schlegel W, Winiger BP, Mollard P, Vacher P, Wuarin F, Zahnd GR, Wollheim CB, Dufy B (1987) Oscillation of cytosolic Ca^{2+} in pituitary cells due to action potentials. Nature 329:719–721
48. Simasko SM, Weiland GA, Oswald RE (1988) Pharmacological characterization of two calcium currents in GH_3 cells. Am J Physiol 254:E328–E336
49. Smith PF, Luque EH, Neill JD (1986) Detection and measurement of secretion from individual neuroendocrine cells using a reverse hemolytic plaque assay. Methods Enzymol 124:443–465
50. Snutch TP, Reiner PB (1992) Ca^{2+} channels: diversity of form and function. Curr Opin Neurobiol 2:247–253
51. Snutch TP, Tomlinson WJ, Leonhard JP, Gilbert MM (1991) Distinct calcium channels are generated by alternative splicing and are differentially expressed in the mammalian CNS. Neuron 7:45–57
52. Soong TW, Stea A, Hodson CD, Dubel SJ, Vincent SR, Snutch TP (1993) Structure and functional expression of a member of the low voltage-activated calcium channel family. Science 260:1133–1136
53. Starr TVB, Prystay W, Snutch TP (1991) Primary structure of a calcium channel that is highly expressed in the rat cerebellum. Proc Natl Acad Sci USA 88:5621–5625
54. Stea A, Soong TW, Snutch TP (1995) Voltage-gated calcium channels. In: Noth RA (ed) Ligand- and voltage-gated ion channels. CRC, Boca Raton, Fla., pp 113–151
55. Stutzin A, Stojilković SS, Catt KJ, Rojas E (1989) Characteristics of two types of calcium channels in rat pituitary gonadotrophs. Cell Physiol 26:C865–C874
56. Tanabe T, Takeshima H, Mikami A, Flockerzi V, Takahashi H, Kangawa K, Kojima M, Matsuo H, Hirose T, Numa S (1987) Primary structure of the receptor for calcium channel blockers from skeletal muscle. Nature 328:313–318
57. Tottene A, Moretti A, Pietrobon D (1996) Functional diversity of P-type and R-Type calcium channels in rat cerebellar neurons. J Neurosci 16:6353–6363
58. Tse A, Hille B (1993) Role of voltage-gated Na^+ and Ca^{2+} channels in gonadotropin-releasing hormone-induced membrane potential changes in identified rat gonadotropes. Endocrinology 132:1475–1481
59. Wang G, Dayanithi G, Kim S, Hom D, Nadasdi L, Kristipati R, Ramachandran J, Stuenkel EL, Nordmann JJ, Newcomb R, Lemos JR (1997) Role of Q-type Ca^{2+} channels in vasopressin secretion from neurohypophysial terminals of the rat. J Physiol (Lond) 502:351–363
60. Zong S, Yassin M, Tanabe T (1995) G-protein modulation of α_{1A} (P/Q) type calcium channel expressed in GH_3 cells. Biochem Biophys Res Commun 215:302–308